

SCALED MOMENTUM SPECTRA IN DEEP INELASTIC SCATTERING AT HERA*

BEATA BRZOWSKA

University of Warsaw, Institute of Experimental Physics
Hoża 69, 00-681 Warsaw, Poland

(Received December 15, 2009)

Charged particle production has been studied in deep inelastic scattering (DIS) using an integrated luminosity of about 0.44 fb^{-1} taken with the ZEUS detector at HERA. The fragmentation properties of the struck quark in deep inelastic scattering have been investigated in the current fragmentation region of the Breit frame as a function of the exchanged boson virtuality Q^2 . The measured evolution of scaled momentum distributions are compared to next-to-leading order calculations convoluted with the fragmentation functions obtained from e^+e^- experiments. Scaling violations are observed. The scaled momentum spectra are also compared to predictions based on a modified leading-logarithmic QCD approximation and Monte Carlo event generators.

PACS numbers: 25.75.Dw

1. Introduction

Quark fragmentation has been studied experimentally in deep inelastic ep scattering at HERA, using observables such as multiplicity moments, scaled momentum distributions and fragmentation functions. The results are usually compared to those obtained in e^+e^- annihilation. In general, universal behaviour has been established and scaling violations of the fragmentation functions observed. It has also been observed that perturbative Quantum Chromodynamics (pQCD) calculations using the modified leading-log-approximation (MLLA) and assuming the local parton-hadron duality (LPHD) do not provide a full description of the data.

Multiplicity distributions of charged hadrons in the current region in the Breit frame¹ are presented as functions of the scaled momentum $x_p = 2P_{\text{Breit}}/Q$ and the variable $\ln(1/x_p)$ in bins of the virtuality of the exchanged boson, Q^2 . P_{Breit} denotes the momentum of a hadron in the Breit frame.

* Presented at the XXXI Mazurian Lakes Conference on Physics, Piaski, Poland, August 30–September 6, 2009.

¹ The Breit frame is defined as the frame in which the four-vector of the exchanged photon becomes $(0,0,0,-Q)$.

The data presented here were collected with the ZEUS detector at HERA between 1996 and 2007 and correspond to an integrated luminosity of 0.44 fb^{-1} . During 1995–97 (1998–2007) HERA operated with protons of energy $E_p = 820 \text{ GeV}$ (920 GeV) and electrons² of energy $E_e = 27.5 \text{ GeV}$, resulting in a centre-of-mass energy of $\sqrt{s} = 300 \text{ GeV}$ (318 GeV).

The tracks used in the analysis had to be associated with the primary interaction vertex and were required to be in the region of high Central Tracking Detector (CTD) acceptance, $|\eta| < 1.75$, where $\eta = -\ln(\tan \theta/2)$ is the pseudorapidity of the track in the laboratory frame with θ being the polar angle of the measured track with respect to the proton direction. The tracks had to pass through at least three CTD superlayers and were required to have a transverse momentum, $P_{\text{T}}^{\text{track}} > 150 \text{ MeV}$.

The analysis of the scaled momenta was restricted to $Q^2 > 160 \text{ GeV}^2$. A well reconstructed neutral current DIS sample was selected by requiring additional cuts reducing background from other processes and giving better reconstruction of events.

2. Theoretical background

The NLO calculations, considered here, combine the full NLO matrix elements with the NLO fragmentation functions obtained from fits to e^+e^- data [1–4]. The MLLA calculations [5] describe parton production in terms of a shower evolution. They depend on two parameters only, the effective QCD scale, Λ_{eff} , and the infrared cutoff scale, Q_0 , at which the parton cascade is stopped. The calculations intrinsically include colour coherence and gluon interference effects. Both leading collinear and infrared singularities are removed and energy-momentum conservation is obeyed. To connect predictions at the parton level to experimental hadron-level data, LPHD [6] was assumed, which leaves only one free parameter — the hadronisation constant, K_{h} describing connection between parton and hadron spectra. The conversion from energy to momentum spectra for the final-state hadrons is performed assuming an effective hadron mass, $m_{\text{eff}} = Q_0$ [7].

Several Monte Carlo (MC) models were compared to the data. Neutral current DIS events were generated using the leading-order QCD ARIADNE 4.12 program [8] including the colour-dipole model. Additional samples were generated with the MEPS model of LEPTO 6.5 [9]. Both MC programs, ARIADNE and LEPTO, are used with the DJANGO 1.1 [10] interface and QED radiative effects are included using the HERACLES 4.6.1 [11] program. Both MC programs use the Lund string model [12] for hadronisation. Hadrons are considered stable if their lifetime is larger than $3 \times 10^{-11} \text{ s}$ and their decay products are not considered.

² The term “electron” is used for both electrons and positrons.

3. Scaled momentum spectra

Scaled momentum distributions were measured as a function of Q^2 in the kinematic ranges $160 < Q^2 < 40960 \text{ GeV}^2$ and $0.002 < x < 0.75$, where x is the Bjorken scaling variable. The inclusive normalised cross-section, $1/N dn^\pm/d\ln(1/x_p)$, with N being the number of events and n^\pm being the number of charged particles, is shown in Figs. 1–2 as a function of Q^2 , together with the published ZEUS results³ in the range $10 < Q^2 < 160 \text{ GeV}^2$ [13].

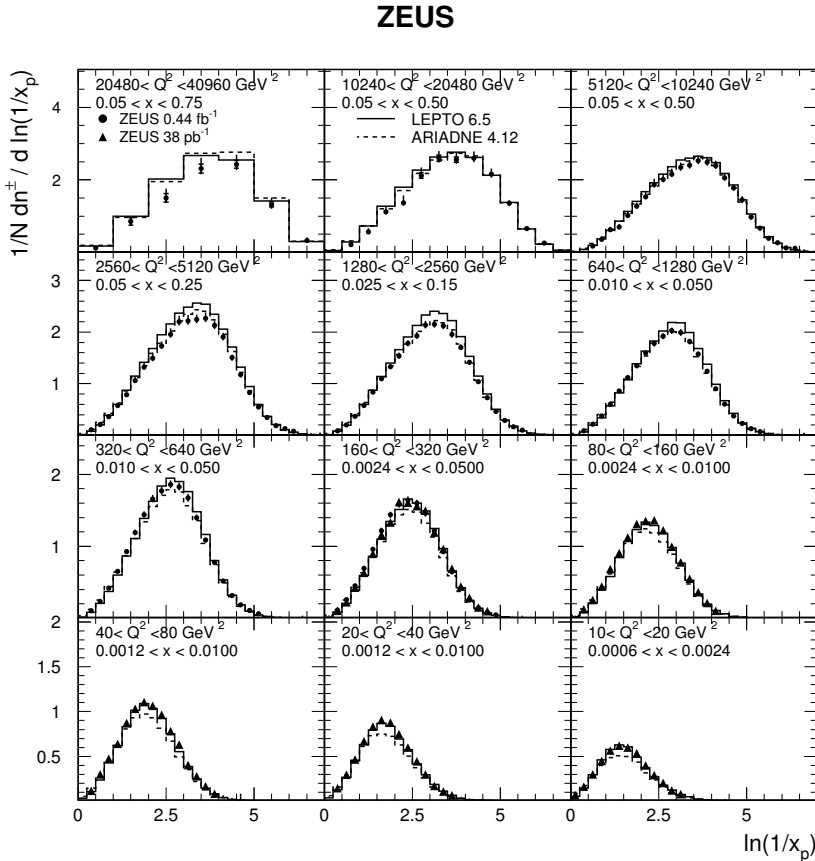


Fig. 1. The scaled momentum spectra, $1/N dn^\pm/d\ln(1/x_p)$, in (x, Q^2) bins. The dots represent the new, the triangles the previous ZEUS measurement [13]. The inner error bars, where visible, indicate statistical uncertainties, the outer statistical and systematic uncertainties added in quadrature. The full and dashed lines represent the LEPTO and the ARIADNE predictions, respectively.

³ The previously published results in the overlap region $160 < Q^2 < 5120 \text{ GeV}^2$ of the two data sets are in good agreement with the new ones. They are not shown except for $160 < Q^2 < 320 \text{ GeV}^2$ in Fig. 1.

These scaled momentum distributions exhibit so-called hump-backed form with an approximately Gaussian shape around the peak [18]. The mean charged multiplicity is given by the integral of the distributions. As Q^2 increases, the multiplicity increases and, in addition, the peak of the distribution moves to larger values of $\ln(1/x_p)$.

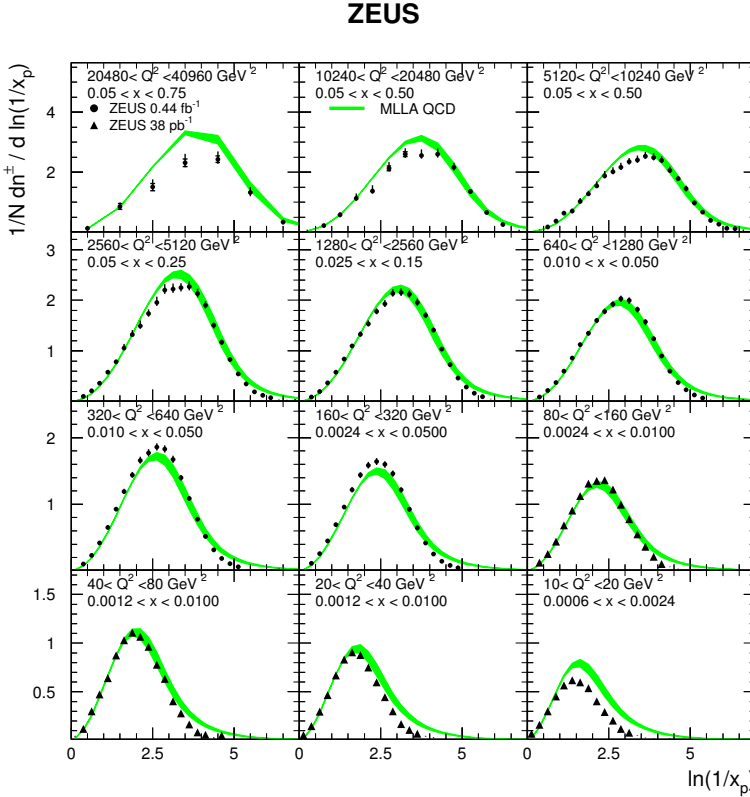


Fig. 2. The scaled momentum spectra, $1/N dn^\pm/d\ln(1/x_p)$, in (x, Q^2) bins. The band represents the range of the MLLA+LPHD predictions. Other details as in Fig. 1.

In Fig. 1, the predictions of ARIADNE and LEPTO are compared to the data. They reproduce the main features of the data with some exceptions. At the highest Q^2 , both models exceed the data at medium and high values of x_p . At medium Q^2 , LEPTO overestimates the data. At low Q^2 , ARIADNE underestimates the data.

In Fig. 2, the data are shown together with MLLA+LPHD predictions [5]. The range for the predictions represents the uncertainties in the input parameters as determined from LEP results: $Q_0 = A_{\text{eff}} = 270 \pm 20$ MeV and $K_h = 1.31 \pm 0.03$. These uncertainties are conservative.

The predictions give a reasonable description of the shapes at $40 < Q^2 < 10240 \text{ GeV}^2$, except for the long tails at high $\ln(1/x_p)$ predicted but not seen at low Q^2 . The tails arise due to inclusion of a mass correction [14] in the calculations. At the lowest Q^2 , the average multiplicity is lower than predicted by MLLA+LPHD. This can be interpreted as a significant migration of particles to the target region of the Breit frame as was also previously observed [15]. For higher Q^2 , the observed shift of the peak positions towards higher values of $\ln(1/x_p)$, is reproduced by the MLLA+LPHD prediction and can be understood within this model as an effect of soft gluon coherence. For the highest Q^2 , the prediction overshoots the data. The ratio of the multiplicities at HERA and LEP decreases with increasing Q^2 [16]. This is reflected in the MLLA predictions using the LEP data as input. The resulting discrepancy with HERA data has also been observed by the H1 experiment [16].

4. Scaling violation

As the energy scale, Q , increases, the phase space for soft gluon radiation increases, leading to a rise of the number of soft particles with small x_p . These scaling violations can be seen when the data are plotted in bins of fixed x_p as a function of Q^2 .

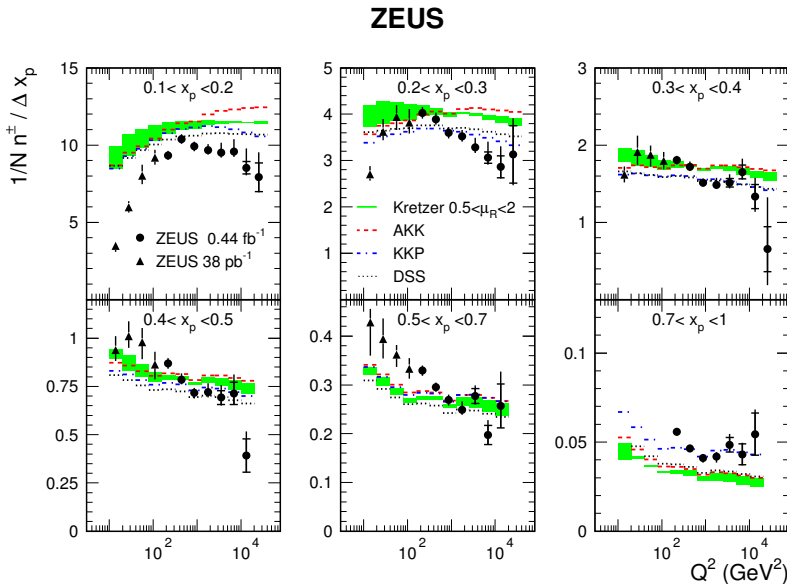


Fig. 3. The normalized number of charged particles, $1/N n^\pm/\Delta x_p$, as a function of Q^2 in x_p bins as indicated. The shaded band represents the NLO calculation by Kretzer [1] with its renormalisation scale uncertainty. Additional NLO calculations are shown: Kniehl, Kramer and Pötter [2] (KKP), Albino, Kniehl and Kramer [3] (AKK) and De Florian, Sassot and Stratmann [4] (DSS).

Figure 3 shows the data together with the NLO+FF QCD predictions [1–4] which were tuned to e^+e^- data. The fragmentation functions were obtained for $x_p > 0.1$, where theoretical uncertainties are small.

The predictions based on all four fragmentation functions are similar in shape. Theoretical uncertainties of all model predictions are similar in size and are only illustrated for Kretzer’s calculations [1]. The models roughly describe the general features of the data. This includes the decrease of the multiplicities from the smallest to the largest x_p by two orders of magnitude. The general trends of scaling violations as a function of Q^2 are also roughly described for all the x_p bins. However, all NLO calculations significantly differ from data. In general, scaling violations are underestimated.

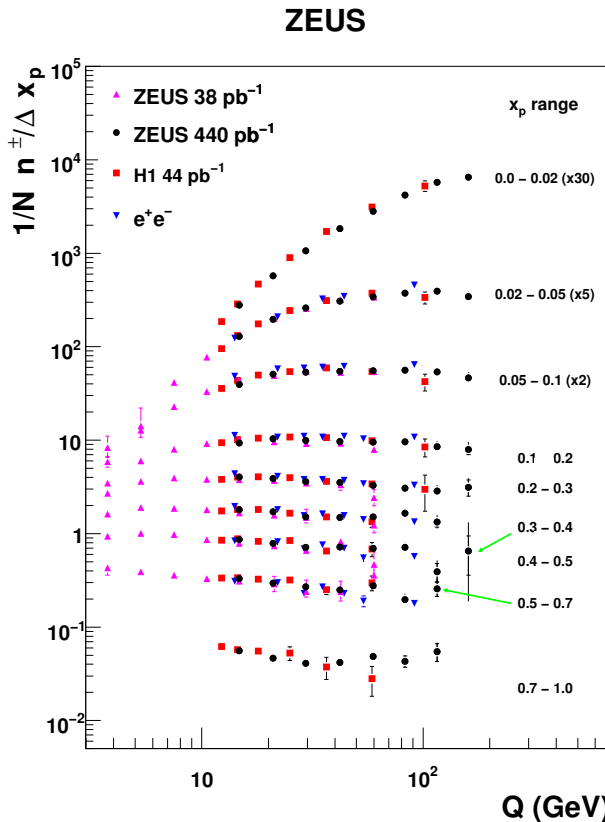


Fig. 4. The normalized number of charged particles, $1/N n^\pm/\Delta x_p$, as a function of Q in x_p bins as indicated. Also shown are the data from H1 [16] and e^+e^- [17]. The dots (triangles) represent the new (previous [13]) ZEUS measurement, the squares the H1 data and the inverted triangles the e^+e^- data. The inner error bars, where visible, indicate statistical uncertainties, the outer statistical and systematic uncertainties added in quadrature. The three lowest x_p bins are scaled by factors of 30, 5 and 2, respectively.

Figure 4 shows the inclusive normalised cross-section, $1/N dn^\pm/dx_p$, as a function of Q in bins of x_p . The data are compared to the results from H1 [16] and from e^+e^- experiments [17]. For the e^+e^- experiments, the scale is taken to be $Q = 2 E_{\text{beam}}$, where E_{beam} is the beam energy. The overall agreement between the different data sets shown in Fig. 4 supports fragmentation universality.

5. Conclusions

Scaled momentum spectra have been measured in NC DIS for the current region in the Breit frame over the large range of Q^2 from 10 GeV² to 40960 GeV². They show clear evidence of scaling violation in a single experiment. Comparing the data to e^+e^- results generally supports the concept of quark-fragmentation universality. Neither MLLA+LPHD nor NLO+FF calculations describe the data well. The MC models ARIADNE and LEPTO need to be improved to reproduce the measured data.

I wish to thank the Mazurian Lakes Conference Organizers for a friendly atmosphere. I am grateful for discussions with W. Khoze, W. Ochs and R. Sassot. Special thanks go to S. Albino for providing the QCD calculations. Research work is co-sponsored from means of the European Social Funds and Budget of Poland within the Integrated Operative Program of Regional Development, Operations 2.6 “Regional Innovative Strategy and Transfer of Knowledge”, personal project of the Mazovian province called “Mazovian Scholarship for PhD students”.

REFERENCES

- [1] S. Kretzer, *Phys. Rev.* **D62**, 054001 (2000).
- [2] B.A. Kniehl, G. Kramer, B. Pöter, *Phys. Rev. Lett.* **85**, 5288 (2000).
- [3] S. Albino *et al.*, *Nucl. Phys.* **B803**, 42 (2008).
- [4] D. De Florian, R. Sassot, M. Stratmann, *Phys. Rev.* **D76**, 074033 (2007).
- [5] V.A. Khoze, W. Ochs, *Int. J. Mod. Phys.* **A12**, 2949 (1997); Y.I. Dokshitzer *et al.*, *Basics of Perturbative QCD*, Editions Frontières, Gif-sur-Yvette, France 1991.
- [6] Y.I. Azimov *et al.*, *Z. Phys.* **C27**, 65 (1985).
- [7] V.A. Khoze, S. Lupia, W. Ochs, *Phys. Lett.* **B386**, 451 (1996).
- [8] L. Lönnblad, *Comput. Phys. Commun.* **71**, 15 (1992).
- [9] G. Ingelman, A. Edin, J. Rathsman, *Comput. Phys. Commun.* **101**, 108 (1997).

- [10] K. Charchula, G.A. Schuler, H. Spiesberger, *Comput. Phys. Commun.* **81**, 381 (1994).
- [11] A. Kwiatkowski, H. Spiesberger, H.-J. Möhring, *Comput. Phys. Commun.* **69**, 155 (1992).
- [12] B. Andersson *et al.*, *Phys. Rep.* **97**, 31 (1983).
- [13] J. Breitweg *et al.* [ZEUS Collaboration], *Eur. Phys. J.* **C11**, 251 (1999).
- [14] P. Dixon, D. Kant, G. Thompson, *Nucl. Part. Phys.* **25**, 1453 (1999).
- [15] M. Derrick *et al.* [ZEUS Collaboration], *Z. Phys.* **C67**, 93 (1995); J. Breitweg *et al.* [ZEUS Collaboration], *Phys. Lett.* **B414**, 428 (1997).
- [16] F.D. Aaron *et al.* [H1 Collaboration], *Phys. Lett.* **B654**, 148 (2007).
- [17] W. Braunschweig *et al.* [TASSO Collaboration], *Z. Phys.* **C47**, 187 (1990); A. Petersen *et al.* [MARK II Collaboration], *Phys. Rev.* **D37**, 1 (1988); P. Abreu *et al.* [DELPHI Collaboration], *Phys. Lett.* **B311**, 408 (1993); Y.K. Li *et al.* [AMY Collaboration], *Phys. Rev.* **D41**, 2675 (1990).
- [18] Y.I. Dokshitzer, V.A. Khoze, S.I. Troian, *Int. J. Mod. Phys.* **A7**, 1875 (1992).